Proceedings of the 42nd International Conference on Ocean, Offshore and Arctic Engineering
OMAE 2023
June 11- 16, 2023, Melbourne, Australia

OMAE2023-103266

WIND TURBINE LOAD MONITORING DURING MODEL-TEST IN A WAVE BASIN

Sébastien Gueydon*
O3 Engineering Consulting
Sole trader
Springwood, NSW 2777
Australia
Email: sgueydon@msn.com

Ilmas Bayati
Head of Floating Wind
PEAK Wind
Mikkel Bryggers Gade 4, 1460
Copenhagen, Denmark
iba@peak-wind.com

René Bosman
Measurement Systems
MARIN
Wageningen, 6701 AA
The Netherlands
R.Bosman@marin.nl

Wouter van Kampen
Measurement Systems
MARIN
Wageningen, 6701 AA
The Netherlands
W.v.Kampen@marin.nl

Erik-Jan de Ridder
Offshore
MARIN
Wageningen, 6701 AA
The Netherlands
E.d.Ridder@marin.nl

ABSTRACT

For the testing of floating wind turbines in a wave basin, several methods have been developed to include the wind turbine loads acting on the floating foundation. To simplify, there is one main choice for the modelling of the wind turbine loads at the scale of the basin: using a physical rotor in a wind field, or using hybrid methods where the wind turbine loads are computed and applied by actuators to the model. Each approach aims at reproducing the loads that the wind turbine generates at the Froude scale chosen for the construction of the model. Transferring these loads can therefore be seen as a step that is common to all methods. While these loads are essential for the modelling of the wind turbine and its interaction with the floating foundation, they are not yet systematically measured nor reported in all basin tests of a floating wind turbine. Most surprisingly, the benefit of measuring of the wind turbine loads transferred to the floating foundation are not explicitly mentioned in the main guidelines on how to test floating wind turbines [e.g.: ITTC]. This paper gives some examples of diverse test set-ups where these loads are measured and it explains how the wind turbine thrust is analytically retrieved from these measurements. It also emphasizes why monitoring the loads actually transferred to the floater adds up to the quality of the test results and confidence in the experiments.

NOMENCLATURE

DNV-GL Det Norkse Veritas - Germanischer Lloyds.
DOF Degree of freedom
FOWT Floating Offshore Wind Turbine.
ITTC International Towing Tank Committee.
MARIN Maritime Research Institute of The Netherlands.
MaRINET2 Marine Renewable Infrastructure Network for Enhancing Technologies 2.
PSD Power Spectrum Density.
RPM Rotation per minute.

INTRODUCTION

The experimental study of floating wind turbines in wave basins has brought a tide of new developments to the basin model-testing methodology in the last decade ([1]). From performance scaling of the rotor to hybrid testing, new approaches to

*Address all correspondence to this author.

extend the modelling of the loads accounted for in model-tests to the wind turbine loads have been highly refreshing and a source of inspiration for progress in other area of testing: for instance, performance scaling is applied to tidal turbines ([2]), hybrid testing is used for the modelling of innovative mooring systems (ongoing work at MARIN) and the inclusion of current loads ([3]). The trend to use actuators for the emulation of new types of loading next to the wave loads in a wave basin is meant to last. It is undeniable that the use of actuators provide a good and simple solution to emulate other loads than hydrodynamic loads in a wave basin. Off the shelves products (like ducted thrusters, drones) of the aeronautical modeling industry are affordable, robust and light. This motivates many experimental facilities to explore new applications where these products can be used as load actuators (e.g. [4]). Classification's societies and advisory bodies for model-testing have acknowledged this trend and started to issue various documents to assist the investigators in the use of these actuators. Nevertheless, there seems a be a blind corner in this new development: there is no real emphasis on the benefit of measuring the loads in real-time that actuators deliver during the model tests. The recent release of the ITTC technical documentation dedicated to the testing of Marine Renewable Energy devices does not mention it ([5]). The recommended practise on the coupled analysis of floating wind turbines issued by DNV-GL also omits this topic ([6]). There are very few publications that claim to monitor the load produced by actuators and even fewer that shared any record of these loads (e.g.: [7] and [8]). MARIN has been monitoring the loads experienced by the wind turbine quasi-systematically since the very first test of a floating wind turbine (Sway AS in 2007). These loads have been measured in a large variety of set-ups. MARIN is commonly using 6 component load frames as load sensors for this purpose. Figure 1 shows such load frame assembled as part of the original MARIN 5MW scaled wind turbine ([9]). A similar sensor has been used during hybrid testing at multiple occasions with diverse solutions representing the wind turbine. Figure 2 highlights the location of a 6 component load frame underneath the structure representing the wind turbine in an hybrid testing set-up using winches to apply the wind turbine loads. The load sensor is also visible in Fig. 3 where it is used to monitor the loads delivered by ducted fans. The same sensor is again used in Fig. 4 to measure the loads under a drone. The authors would like to motivate other facilities to implement the monitoring of the loads generated by actuators in their test set-up too as they believe that it is an essential step in the quality control of any test where actuators are used. This paper describes test set-ups where actuators have been used and their loads monitored. It explains how these loads are measured and proposes an analysis method to extract the wind turbine loads from the load measurements.

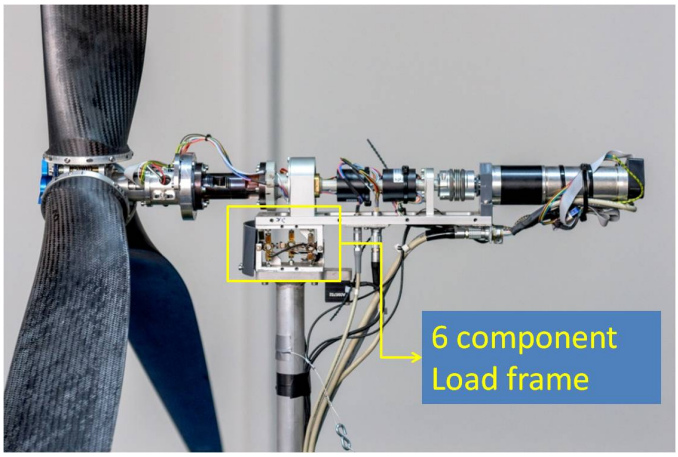

FIGURE 1. MARIN 5MW SCALED WIND TURBINE AT SCALE 1/50

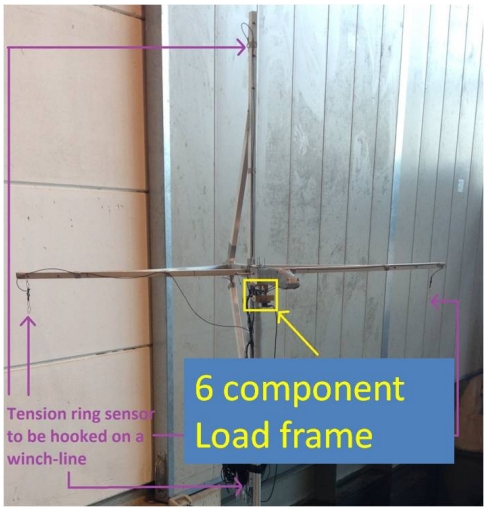

FIGURE 2. MARIN WINCH-SYSTEM

MEASUREMENTS OF LOADS AT THE TOWER-TOP

Load frames come in different sizes and measurement ranges. Nevertheless, they can all be described as a clever assembly of transducers. Their arrangement and the deformation of the frame makes it possible to retrieve up to 6 components of the global load exerted on the frame following simple arithmetic relations. The force transducers are assembled on the bottom and top plate with flexure hinges in between transducers and the plates to prevent any stick slip in the load measurements (e.g. Fig. 5). By accounting for the position and orientation of each individual sensor, the loads recorded by the distinct sensors are combined to determine the global loads exerted on the frame at its geometrical centre. In addition to the calibration data of all

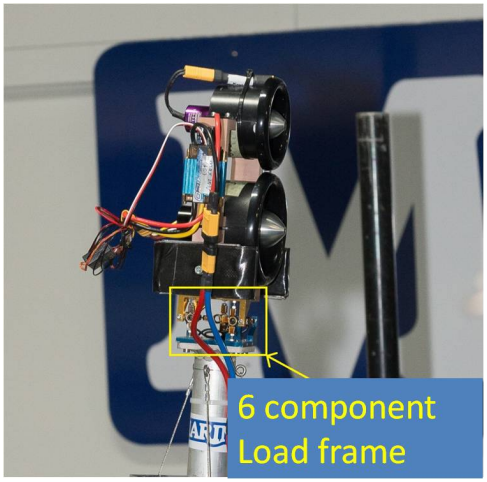

FIGURE 3. MARIN FAN-SYSTEM

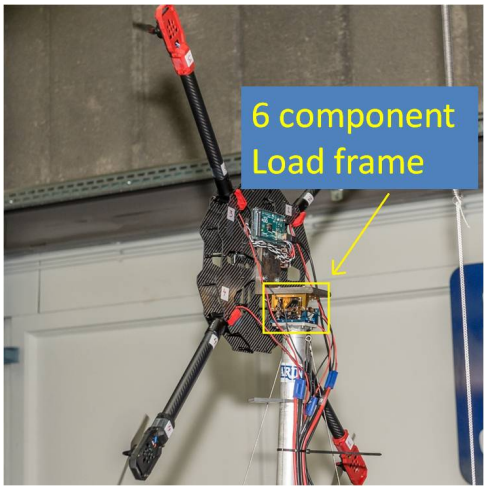

FIGURE 4. CENER DRONE-SYSTEM

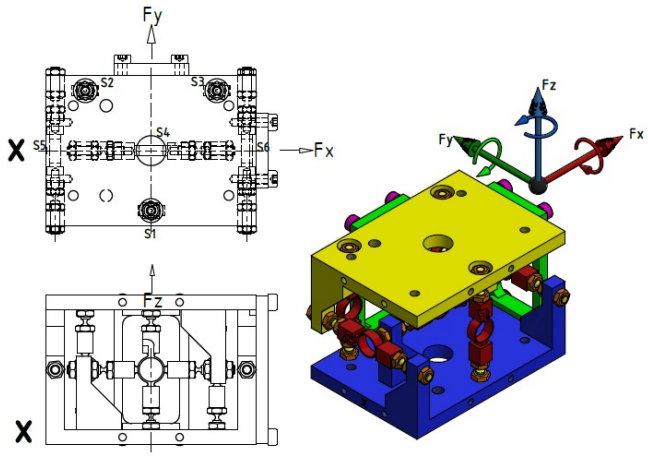

FIGURE 5. 6 COMPONENT LOAD FRAME

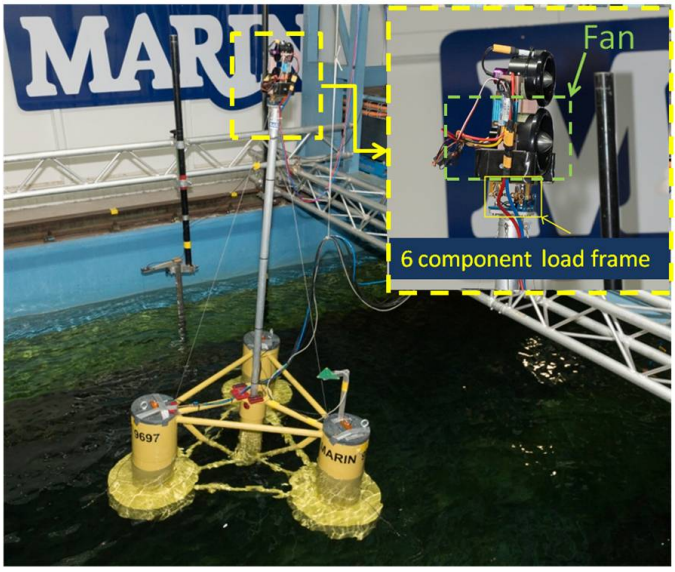

FIGURE 6. DeepCwind semisubmersible with a ducted fan

individual sensors, the calibration of the whole load frame is required. This makes it possible to account for the deformation of the frame under loading in the conversion of the reading of the force measured by the sensors to the 6 components of the global load on the frame.

FLOATING WIND TURBINE MODEL

For this paper, the model of a wind turbine used in a test campaign in the Concept Basin of MARIN in the fall 2019 has been chosen as an illustration of how the turbine loads can be monitored and analyzed. The description of the full set-up is publicly available in [10]. The picture of the test set-up is shown in Fig. 3. The wind turbine loads were emulated by a ducted fan mounted at the top of a very stout tube representing the rigid tower. To further increase the rigidity of this tower, 3 guy wires were tensioned between the top of the tower and the columns of the semisubmersible. The force balance of Fig. 5 was placed between the tower and the actuator generating the thrust. In this example, the load frame of Fig. 5 was used to monitor the 3 forces Fx, Fy, Fz and 3 moments Mx, My, Mz at the connection of the fan and the tower-top. It has been engineered, designed and manufactured by MARIN for the purpose of model-testing. The uncertainty on the measurement of Fx by this frame is below 0.5% of the applied Fx in the range of 10 N to 220 N.

As visible on the photography of Fig. 6, two ducted fans were mounted on the tower for this test campaign. MARIN ceased the opportunity to check individually the performance of two fans in the same model-test campaign. The fans were not operated simultaneously. The results presented in this paper were obtained with the bottom fan, which is the biggest and most powerful of the two fans. This fan is produced by WeMoTech for remote control (RC) aeroplane models. It consists of a motor and a multi-bladed fan. It was selected based on the range of thrust that it can deliver and its robustness. An RC sensor was added to monitor the rotation speed of the fan's motor. The voltage is directly related to the rotation speed of the motor. The output of the sensor is converted to a speed and read from an LCD screen. This set-up has exclusively been used in this campaign to do tests at constant levels of thrust. The thrust was achieved by providing a voltage to the motor speed.

All the electrical components of the fan were powered by a voltage supply installed on the side of the basin. This external power supply was preferred to batteries for safety reasons. The power supply could easily be switched off with an emergency stop. Additionally this solution has also the advantage of guaranteeing a stable voltage supply and thus a stable rotation speed of the fan. However, the power cable needs to be carefully selected. It needs to be suitable for the required current and gives a minimum voltage loss over its length. Therefore it needs to be thick enough but not too thick such that its weight and lack of flexibility don't disturb the motion of the floater.

Prior to the tests in the basin, the fan system with its load frame was placed on a fixed structure and tested to obtain the relation between the motor's rotation speed (RPM) and delivered thrust. Calibration data are shown while compared to the thrust measured during the actual testing (Fig. 15). During this calibration work, the repeatability of this relation was verified. It was also checked that the system can deliver a stable thrust for longer than 25 min, which is a typical duration of tests at the considered scale of 1/50. With the availability of trustworthy calibration data, measuring the loads may seem unnecessary as the thrust follows from the RPM measurement. Nevertheless, monitoring the actual thrust delivered by the fan gives more options. It enables to check that the relation between RPM and thrust which was determined from steady measurements in static conditions (i.e. the fan was fixed during the calibration) are still valid in dynamic conditions where the floater and the fan are moving with rpm-controlled setting. It also makes it possible to use the thrust as control parameter rather than the fan's rotational speed. The latest option is the most suitable for hybrid testing during which the thrust is dynamically calculated by a software while the tests are ongoing. However, this supposes that the thrust can be retrieved from the load measurements of the 6 component load frame. Furthermore the dynamics of the fan system must be able to follow this calculated thrust set point.

EXTRACTION OF AERODYNAMIC LOADS

The total aerodynamic loads acting on a wind turbine in operation comprises the thrust generated by the rotor, and drag forces acting on the tower and the part of the foundation exposed to wind. For an operating rotor, the thrust is much larger than these drag loads. For simplification, only the thrust is considered in this study and the drag loads on other elements than the rotor are neglected. Therefore, in Fig. 7 and all following figures the load extracted from the actuator's force in x direction is assimilated to the thrust of the emulated wind turbine. On top of the aerodynamic loads, the gravity loads and the inertial loads need to be considered to match the total loads experienced by the turbine.

Figure 7 shows the sketch of a single ducted fan mounted on a load frame at the top of a tower. Several locations are of importance for the transfer of the loads from the fan to the floater via the tower.

H: the hub centre which can also be considered as the centre of mass of the fan alone for simplification,
G: the centre of mass of the fan system which is made of the fan, a mounting plate, a portion of the load frame, possibly other components for the power supply and control of the fan, and sometimes ballast weights,
N: the middle of the load frame which is considered as the interface point of the nacelle where the 6 components of the loads are measured.

It is capital to realize from Fig. 7 that the loads exerted by the fan (at H) are not directly the loads measured by the load sensors (at N). For instance, the thrust force applied at H generates a moment at N. So does the total weight of the whole fan system too for which the arm depends on the distance GN. For the inertia moments of the fan system to be considered, these need to include those of the fan itself and those of all other components. These moments should eventually be expressed at the centre of the load frame N. Once transferred to N, the inertia matrix of the whole fan system will most certainly includes non-diagonal components (especially coupling terms between surge and pitch). Such that the construction of the fan system is at the origin of a discrepancy of the loads generated by the fan and those measured by the 6 component load frame. The load frame does not exclusively measured the loads generated by the fan, but also the weight and inertial loads. Fortunately, these components can be determined and subtracted from the total measured loads; leaving the exclusive contribution of the fan. This chapter explains how this was done in this campaign.

As it is common practice for most sensors, the signals of the 6 component load frame are zeroed at the start of the model-tests. This is cancelling all steady load components, like those caused by the weight. Nevertheless, the components that vary with the motions, like the projection of the weight along the x, y and z axes and the related moments are still contributing to the total

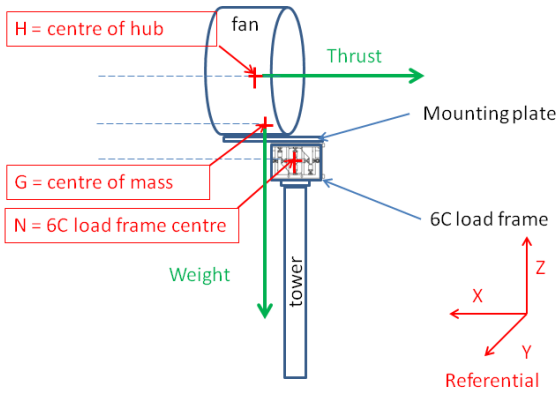

FIGURE 7. Schematic description of the load transfer from a ducted-fan

loads captured by the load frame. Knowing the mass of all elements above the load frame, the dynamic weight components can be calculated using the monitored roll and pitch rotation angles. The associated moments were obtained by multiplying this weight with the arm formed between the centre of mass of all elements above the load frame and its geometrical centre N. The inertial forces are equal to the product of the same mass by the accelerations at the centre of the load frame. The inertial moments are the product of the gyration moments by the rotational accelerations. The accelerations around the x-axis, y-axis and z-axis can be derived from the combinations of the translation accelerations at 3 positions on the rigid floater. Once, the translation accelerations measured at any of the 3 accelerometers are transferred to the centre of the load frame, the 6 components inertial loads acting on the load frame can be determined when the floater, the tower and the nacelle are all considered as part of the same rigid body. Within this assumption of full body rigidity, the present set-up provides us with everything we need for the extraction of the weight loads and inertial loads acting on the load frame. In this way, the remaining loads are the contributions caused by the operating fan. These remaining components represent the aerodynamic loads acting at the top of the wind turbine's tower (more precisely at location N).

The extraction of the actual loads due to the fan is an analytical exercise which requires a very detailed knowledge of the assembly of all components of the fan system. In particular, the inertia properties of the fan system can be difficult to assess with sufficient certainty. Three main paths can be followed for their assessment. The first one is rely on detailed technical drawings of all components (or Computed Assisted Design data). The second one is to experimentally determined the centre of mass and inertia moments of the part(s) of the fan system. This can be done through swing tests for instance. The third way is to choose simplified geometry for all or parts of the components (e.g. represent the ducted-fan by a cylinder) and assemble all these inertia moments to an estimated total inertia 6x6-matrix at the centre of mass of the whole system G of Fig. 7. Whatever the way the total inertia matrix is determined, it remains an estimation process which results should be considered with some precaution. Thankfully, these estimates can be checked and even refined against model-test results. Some tests are providential to verify the estimated values of the inertia matrix:

1. Static load tests: the test designed to check the mooring restoring loads to a pitch inclination can provide steady moments monitored in the load frame and their relation with the pitch angle. This enables to check the total mass acting on the load frame and the position of the centre of mass of the fan system.
2. Hydrostatic tests: the test designed to check the longitudinal metacentric distance (GML) of the whole floater can provide steady measurement from the load frame and their relation with the pitch angle. This enables to check the total mass acting on the load frame and the position of the centre of mass of the fan system.
3. Surge decay tests: the knowledge of the acceleration in surge combined with the loads monitored in the load frame makes it possible to verify what the inertia contribution in the force acting in surge is and thus check the estimated mass.
4. Pitch decay tests: the knowledge of the pitch angle and the acceleration in pitch combined with the loads monitored in the load frame makes it possible to verify what the inertia contribution in the pitch moment at N is and thus check some values of the inertia matrix.
5. Tests in still water under constant thrust: the relation between the pitch angle and value of the thrust should corroborate the results of the static calibration of the fan. Knowing the thrust and thus the pitch moment at N, the moment caused by the weight is the other remaining component of the pitch moment measured by the load frame (at N).
6. Shutdown tests in still water: these tests consists in switching off the fan after the floater has come to a steady equilibrium position with a constant thrust. What follows this shutdown (of the fan) is a combined surge and pitch decay (with no thrust). The analysis of these decays gives us similar information as what can be obtained from decay tests and tests under constant thrust. A shutdown test is chosen as an example of the load decomposition method in the next chapter.

$$\overrightarrow{F6C_N} = \overrightarrow{Inrt_N} + \overrightarrow{Wght_N} + \overrightarrow{Aero_N} \quad (1)$$

where,
$F6C_N$ = loads monitored by the load sensors (3 forces and 3 moments at N).
$Inrt_N$ = inertial loads (3 forces and 3 moments at N).
$Wght_N$ = Weight loads (3 forces and 3 moments at N).
$Aero_N$ = loads exerted by the fan (3 forces and 3 moments at N).

The expression of inertia and weight tensors of Eqn. (1) will be further detailed using the motions and the inertia matrix of the fan system. For this purpose, the motion at N is introduced as a 6 component vector with the translations in the first 3 rows (surge, sway and heave) and the rotations (in rad) in the last 3 rows (roll, pitch and yaw):

$$\overrightarrow{X_H} = \begin{bmatrix} x \\ y \\ z \\ \phi \\ \theta \\ \psi \end{bmatrix}$$

The inertia are contained in a 6x6 matrix. These notations are conformed to those of many other publications in ship hydrodynamics (e.g. [11]).

$$\overrightarrow{Inrt_N} = I_N.\overrightarrow{\ddot{X}_N} \tag{2}$$

where,
I_N = 6x6 inertia matrix of the fan system expressed at N;
$\overrightarrow{X_N}$ = 6 component motion vector at N (DOFs: surge, sway, heave, roll, pitch and yaw);
$\overrightarrow{\ddot{X}_N}$ = 6 component acceleration vector at N (DOFs: surge, sway, heave, roll, pitch and yaw).

$$\overrightarrow{Wght_N} = I_N(1,1).R.\overrightarrow{g} \tag{3}$$

where,
$I_N(1,1)$ = Mass of the fan system;
R = rotation matrix from the earth fixed referential to the nacelle fixed referential;
$\overrightarrow{g}$ = gravity vector in earth referential (0, 0, -9.81).

The knowledge of the inertia characteristics of the fan system and the (rigid body) motions and accelerations at N is sufficient to calculate the inertial component and weight component of the loads in Eqn. (1). This provides us with a way to retrieve the loads created by the fan as they make the last unknown component of Eqn. (1).

The (total) longitudinal force in the load frame (F6C-x) and the pitch motion (X_5) that have been recorded prior and after a fan-shutdown event are displayed in Fig. 8. This test includes 2 steady states:

1. Prior to the shutdown event, the floater lies in a stable equilibrium under the loading of the constant thrust. Signals in this state are highlighted in green.
2. Well after the shutdown event till the end of the recording, the floater lies in a stable equilibrium with no thrust excitation. Signals in this state are highlighted in red.

The differences (in F6C-x and X_5) between these 2 steady states are exclusively due to the loss of thrust and the change of the longitudinal projection of the weight. Back to Eqn. 1, the inertia term ($Inrt_N$) can be disregarded while the value of the thrust loss is known from calibration data of the fan. Between these 2 steady states, the aerodynamic moment in pitch has disappeared. That informs us on the arm HN of Fig. 7 that contributes to the pitch moment felt in the load frame. In addition, the weight projections in the longitudinal direction (X) and the vertical direction (Z) have changed with the pitch inclination. The variations of weight forces and moment in pitch inform us on the mass of the whole fan system and the arm GN of Fig. 7.

Let's now look at the transient state between the 2 steady states. The records of the longitudinal force in the load frame (F6C-x) and the pitch motion (X_5) from the time which follows immediately the fan's shutdown event exhibit the dynamics of the system. Signals in this transient state are highlighted in purple in Fig. 8. During this section of the test, the inertia loads are significant because the accelerations decrease quickly in the decaying motion of the turbine. Back to Eqn. (1), the aerodynamic loads are now null, leaving only the weight loads and the inertia loads, both loads acting at the centre of mass G of Fig. 7. This gives us an opportunity to check the value of the mass of the fan system and the position of its centre of mass through the determination of $\overrightarrow{GN}$.

Figure 9 shows the decomposition of the forces measured by the load frame (6C) during two time intervals that represents two of the distinct states discussed previously:

1. Prior to the shutdown event when the fan operates at constant RPM in still water and the system lies in equilibrium. All signals highlighted in green in Fig. 8.
2. Right after the shutdown event when the pitch motion decays due to the loss of thrust. All signals in this dynamic state are highlighted in purple in Fig. 8.

The longitudinal load in the load frame can be split in 3 components corresponding to the 3 terms of Eqn. (1):

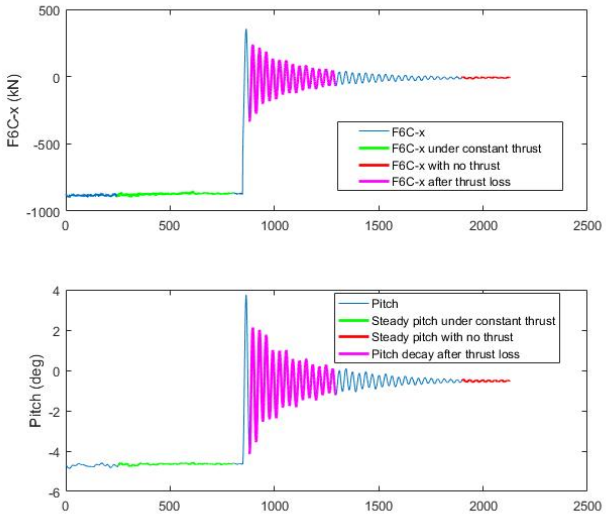

FIGURE 8. PITCH AND LOAD DURING A SHUTDOWN EVENT

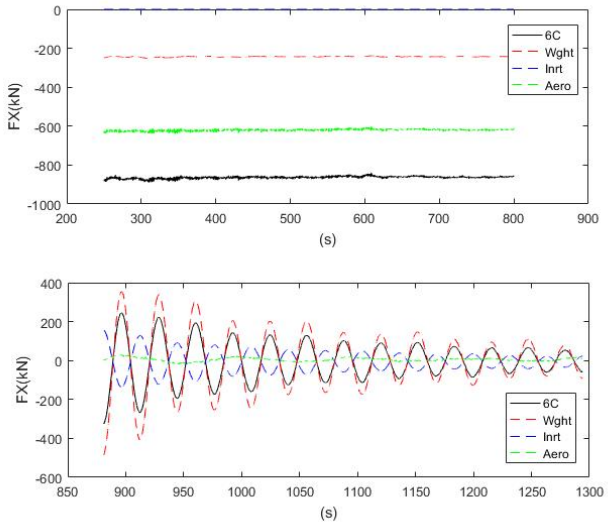

FIGURE 9. LOAD DECOMPOSITION DURING A SHUTDOWN EVENT

'6C' stands for the total measured forces by the load frame,
'Wght' stands for the dynamic contribution of the weight of all elements above the load frame,
'Inrt' stands for the inertial loads of all elements above the load frame,
'Aero' stands for the remaining part that must represents the aerodynamic loads acting on the wind turbine. The aerodynamic load in the x-direction is the thrust of the fan.

Following this decomposition, the thrust appears steady and relatively unaffected by the decaying motion of the floater. It is noted that the absolute mean value of the Fx component as measured by the load frame is much bigger than the actual thrust. This is caused by the projection of the weight that grows with the trim angle of the floater.

This load decomposition is applied to all tests with the fan in operation. Results of this load decomposition are shown for a few of these tests in the next chapter.

REAL-TIME LOAD MONITORING

The hardware and method developed in the previous sections are employed in this section through several examples of tests with the DeepCWind semisubmersible. It is useful to emphasize that the extraction of the wind turbine loads is purely based on the decomposition of all the loads leading the dynamic responses of the part of the wind turbine above the load frame. As such the analysis method does not rely on any filtering technique to isolate the inertia loads or the weight, which makes it applicable to any kind of floaters. The biggest simplification is that it considers the turbine and the floater has a rigid body to be able to easily transform the motions and the acceleration from any location of the floater to the centre of the load frame (points N of Fig. 7). This limitation should not be an issue for floaters with soft responses like spars, semisubmersible platforms and barges which motions are mainly restricted to the wave frequency range or below (i.e. well below the natural frequencies of the tower). Nevertheless it could become an obstacle if the goal of the tests was to investigate specifically the effects of high frequency responses on the floater (e.g. tests in steep and breaking waves with the turbine operating). This simplification might also be too strong for floaters with very stiff motion responses like tension leg platforms which motion modes are likely to merge with the structural modes of the tower ([12]). In this case, a simple fix could be to monitor the accelerations and the motion directly on the load frame such that these measurements include the structural responses of the tower.

Still water tests with constant thrust

This chapter presents results for 7 fixed RPM tests while the floater lays calmly in still water, which Fig. 10 gives an illustration of. At rest, the floater is tilted under the effect of the thrust as can be seen in Fig. 11. Applying the decomposition method of the previous chapter, the thrust can be extracted from the measured longitudinal force Fx 6C in the load frame (Fig. 12). The extracted thrust is not perfectly constant for all these tests but some small variations can be observed at high and low frequencies (standard deviation less than 1.5 percent of mean value).

These small variations have several sources. Firstly, the accelerations are used in the determination of the net aerodynamic thrust from the total load measured by the load frame. Acceleration measurements are noisy due to the vibrations of the structure and the sensors themselves. Another important source of noise is the actuator itself. A spectral analysis of a pitch decay test with the fan operating at 3960 RPM confirms that the fan causes significant vibrations at frequencies higher than the platform's motion frequencies. The spectra of the measured force in surge (6C) and the extracted thrust (Aero) are shown in Fig. 13. The variations measured in the load frame around the surge and pitch eigen frequencies are neatly removed by the load decomposition method as the spectrum of the thrust signal testifies. Nevertheless, an increase of high frequency vibrations was observed when the fan was turned on. This noise induced by the fan has a similar impact on both signals (6C and Aero). In Fig. 13, a broad peak of vibrations is clearly visible around 9 rad/s. This noise occurs at frequencies much lower than the 1P frequency of the fan. The frequency of this peak does not seem to coincide with the tower's eigen frequencies for the first bending mode or the second bending mode. The presence of noise in the thrust signal was not judged detrimental to the demonstration of the method for the extraction of the thrust and therefore no filtering was applied. The mean values of these thrust signals are plotted against the fan's velocity (in RPM) in Fig. 14.

For every fixed RPM tests, the average value of the extracted thrust signal can be compared to the thrust value corresponding to the RPM setting of the calibration curves of the fan alone which was obtained before the tests in the basin. The values of the thrust extracted from the fixed RPM tests with the floater in the basin agree well with the values measured during the calibration of the fan (Fig. 15). This shows that there is no significant variation of the fan's performance between the calibration's set-up and the basin's set-up. The wind turbine thrust emulation is working as expected.

Operational wave with constant thrust

The system of Fig. 6 has been tested in regular and irregular waves with and without thrust ([10]). One of these conditions was a JONSWAP spectrum with peak period T_p of 12.1 s and significant wave height H_s of 7.1 m. Figure 16 shows the Power Spectrum Density (PSD) of different wave realizations of this operational sea-state. 3 Tests were conducted with the fan operating at fixed rotation speed at 3960 RPM, 4650 RPM and 5400 RPM. Figure 17 displays the signals of the thrust processed from the measurement of the load frame as explained in the previous chapter. There again the thrust signals are relatively steady although noisy. The standard deviations of the thrust signals are slightly higher than what has been observed in the still water tests but remains small relative ($< 3\%$) to the thrust mean value (Table 1).

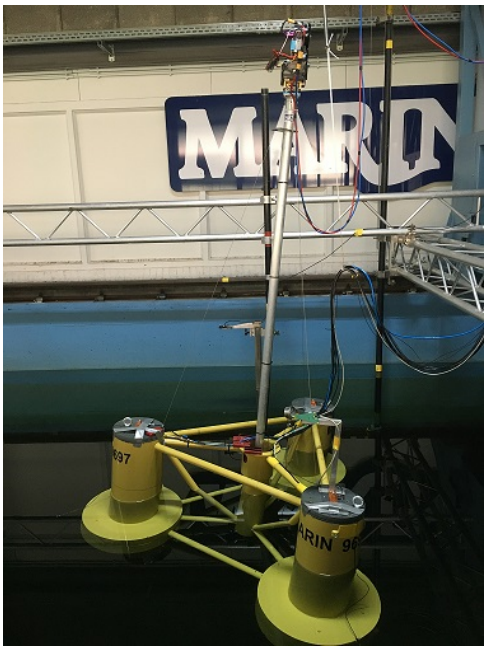

FIGURE 10. CONSTANT THRUST IN STILL WATER TEST

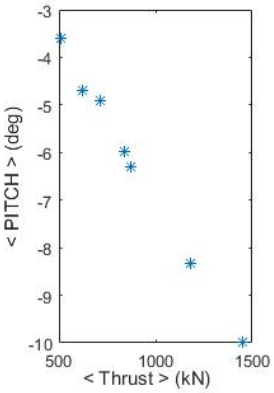

	Mean_deg
3600 rpm	-3.5945
3960 rpm	-4.6934
4260 rpm	-4.9064
4650 rpm	-5.9917
4710 rpm	-6.3085
5400 rpm	-8.3174
6060 rpm	-9.9977

FIGURE 11. PITCH MEAN INCLINATION

BENEFITS OF MEASURING THE THRUST DURING THE MODEL-TESTS

In the previous sections, it has been demonstrated that the thrust can be accurately obtained from the loads measured at the connection point between the nacelle and the tower. Knowing the actual value of the applied thrust is a great asset for several reasons.

Having the option of exerting a given load through an actuator (like a fan) without changing anything to the test set-up makes some usual system's verification and documentation tests easy to

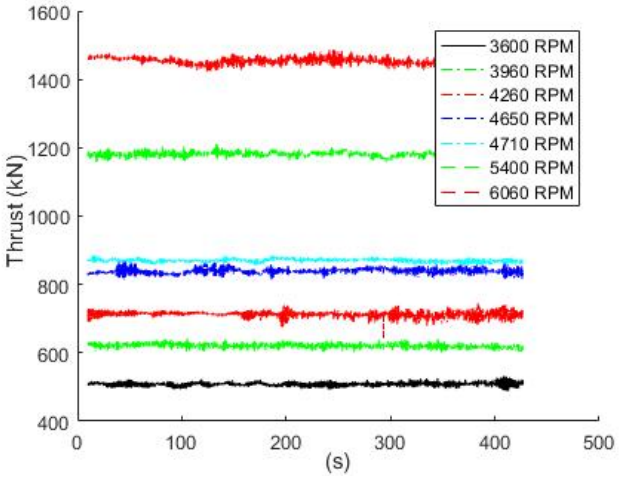

FIGURE 12. ESTIMATION OF THE THRUST SIGNAL

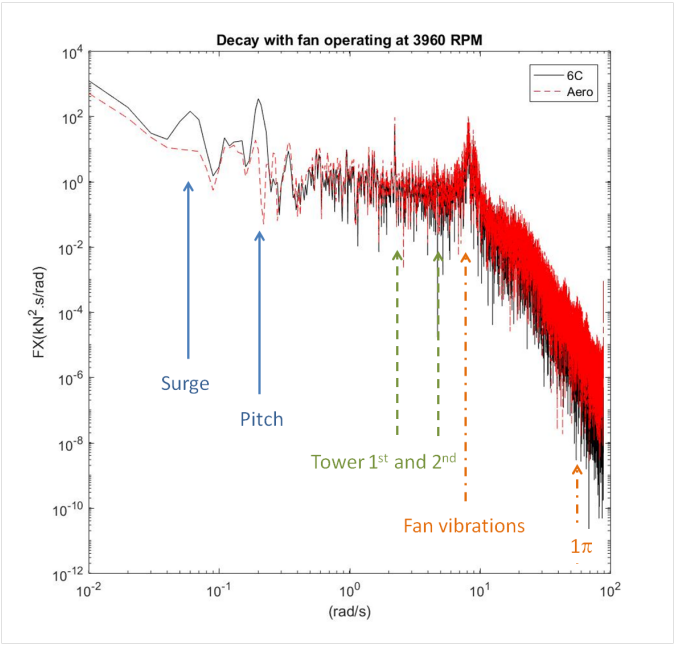

FIGURE 13. PSD OF MEASURED FORCE IN SURGE VERSUS EXTRACTED THRUST

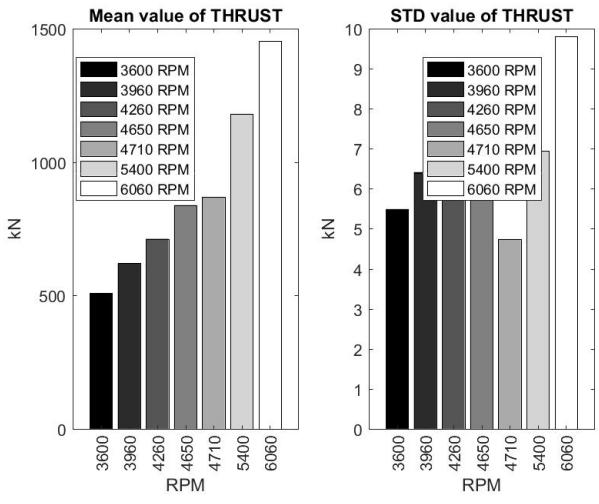

FIGURE 14. THRUST VALUES AS FUNCTION OF FAN'S RPM SETTING

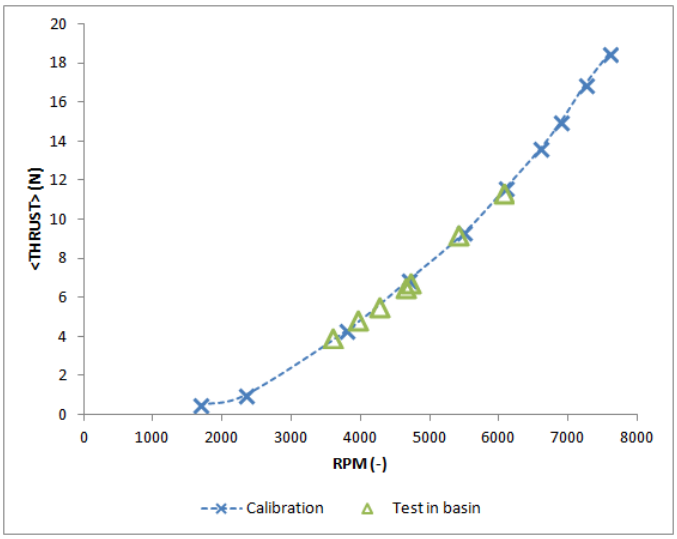

FIGURE 15. THRUST VALUES FROM TESTS IN BASIN AND CALIBRATION OF FAN SYSTEM

execute. Increasing the thrust step-wise or combining a series of constant thrust provide experimental data which can be used to check the hydrostatic and mooring restoring characteristics of the model (e.g. [13], [10]). A shutdown event triggers decaying pitch and surge motions which can be analyzed as such to get information on the natural period of the model and associated levels of damping. Knowing the load applied by the actuator ensures a very good repeatability of the testing conditions (c.f. [13], [10]).

It gives a way to monitor and check the true value of the thrust during the actual testing. By doing that, the operator does not depend any longer exclusively on calibration data that were executed prior to the test with a different and often incomplete set-up (where only the fan system was present without the model). Moreover, these calibration data are usually limited to steady conditions and possibly not covering the whole range of application of the fan (new thrust values can be explored and for a longer duration during the tests than during the calibration). Fur-

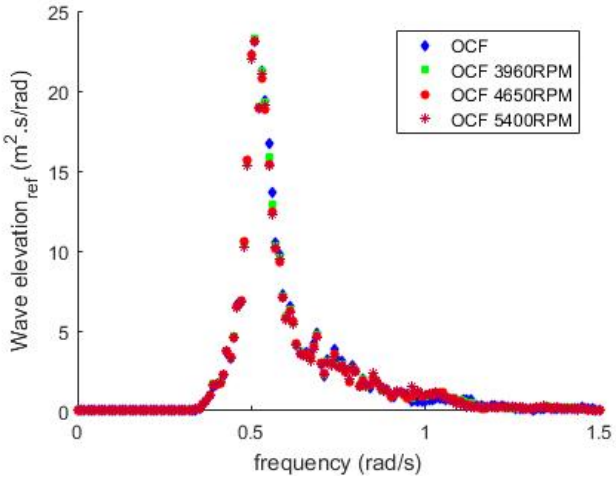

FIGURE 16. OPERATIONAL WAVE SPECTRUM

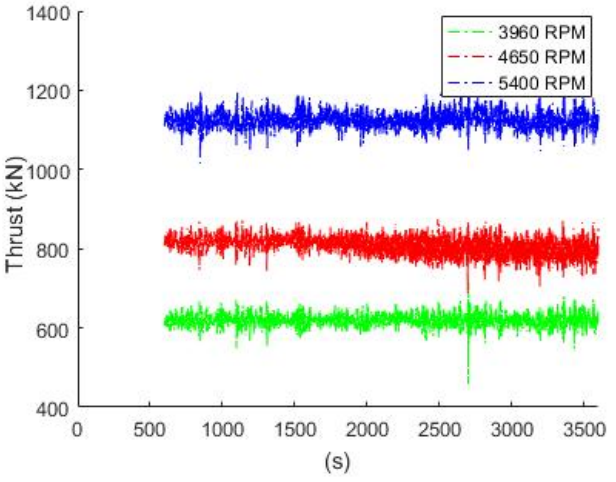

FIGURE 17. ESTIMATION OF THE THRUST SIGNAL

thermore, it gives the possibility to check for any deviation of the performance of the fan over time caused for instance by possible power supply issue, overheating or mechanical wear and tear. These deviations can be easily spotted when the current thrust is monitored. That also enables to assess how much the thrust varies from the requested target value. This is already valuable when testing under constant thrust and even more when the set-point for the thrust varies over time. This is the case in hybrid testing where the wind turbine loads are calculated in live conditions by an aerodynamic software during the test in the basin. The comparison of the loads applied to the physical turbine with the targeted loads calculated by the software gives the most robust quality assurance that the emulation of the wind turbine is properly achieved.

TABLE 1. THRUST STATISTICS IN WAVE TESTS WITH FIXED RPM

RPM setting	Mean	STD	STD/Mean (%)
3960	617.07	17.18	2.78
4650	798.72	22.50	2.82
5400	1121.89	19.82	1.77

In 2018, adjacent to the tests done with the fan system of Fig. 6, a drone system of CENER was mounted on the same floater Fig. 19 and hybrid tests were completed as part of the project ACTFLOW within the 3rd call of the MARINET2 infrastructure transnational access program. The drone system allowed to account for pitch and yaw moments in addition to the thrust as part of the wind turbine loads acting on the floater ([14]). This test set-up is visible in Fig. 4. It used the same load frame as the example previously developed of Fig. 3. Several publications have covered the results of ACTFLOW. MARIN employed the same load monitoring and analysis techniques as presented in this paper to track the wind turbine loads applied by this actuator. This time the drone system was not operating only at constant thrust but also in gust winds with a collection of wind turbine controllers designed specifically for this floating foundation. The control strategies have been developed by POLIMI and TU Delft ([15]). One of this controller was tested in operational waves (same PSD as in Fig. 16) under 3 gust wind conditions with active control. Figure 18 displays the thrust set-point signals in the top graphic and the realized thrust for these 3 tests. Without entering into a detailed comparison, it can be seen that there is a good resemblance between the thrust extracted from the load measurements at the nacelle and the targeted thrust provided by the software. The monitoring of the wind turbine load makes it possible to do this comparison for the thrust and also other moments generated by any actuator.

CONCLUSION

The loads applied by an actuator can be monitored using a 6 component load frame. The theory behind the extraction of the wind turbine loads from the measurements of loads by a 6 component load frame is straightforward. This paper develops the example of how this method was implemented for a semi-submersible floating wind turbine using a fan for the emulation of the wind turbine thrust. It is noted that the same technique can be deployed for other floater types with no to little adapta-

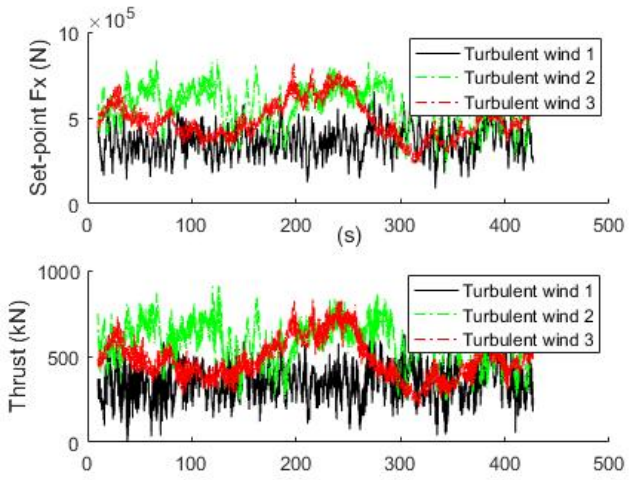

FIGURE 18. ESTIMATED THRUST SIGNAL WITH SEP-POINT SIGNALS

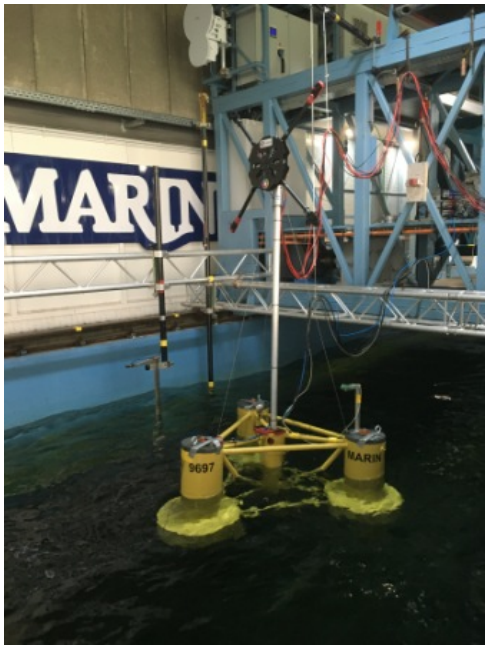

FIGURE 19. DEEPCWIND SEMISUBMERSIBLE WITH THE DRONE SYSTEM OF CENER

tions. Only for some cases (like for a TLP), it is preferable for this method to monitor the motions and the acceleration as close as possible to the load sensor(s). In addition to the improved ease with which some documentation tests can be executed with load actuators (e.g.: static load tests, decay test), the monitoring of the loads delivered by actuators enables to keep an hold on the accuracy and precision of the actuation process. Under achieving load actuators being diagnosed as one of the main risk of hybrid testing ([4]), the authors believe that the monitoring of the actuation loads must be given a higher priority as what they have been commonly given so far. Especially during hybrid testing where the target loads are calculated in real time by a software, the comparison of the delivered loads and the target loads should be systematically done and shared with the customer. This would highlight the performance of the hybrid testing system with no ambiguity.

ACKNOWLEDGMENT

Thanks go to MARIN and all technicians, laboratory operators and other employees involved in the preparation and execution of floating wind turbine model-tests in the last 15 years. We also would like to thank José Azcona and Òscar Pires from CENER who have authorized us to use a picture of their drone system and a plot of ACTFLOW results. Our thanks go to all other participants of this project from POLIMI and TU Delft for their multiple contributions: A. Fontanella, J. Vittori, Y. Liu, J. Wingerden, M. Belloli. MARIN's work on developing new techniques for the testing of floating wind turbines in a wave basin has been sponsored by the Dutch government over many years through the ARD-TKI funds. ACTFLOW was financed by European Union's Horizon 2020 research and innovation programme under grant agreement number 731084, project MaRINET2.

REFERENCES

[1] Bredmose, H., Larsen, S., Matha, D., Rettenmeier, A., Marino, E., and Saettran, L., 2012. *Collation of offshore wind wave dynamics*. 01.

[2] Noble, D. R., Draycott, S., Ordonez Sanchez, S., Porter, K., Johnstone, C., Finch, S., Judge, F., Desmond, C., Santos Varela, B., Lopez Mendia, J., Darbinyan, D., Khalid, F., Johanning, L., Le Boulluec, M., and Schaap, A., 2018. D2.1 Test recommendations and gap analysis report. Tech. rep., MaRINET2, may.

[3] Otter, A., Flannery, B., Murphy, J., and Desmond, C., 2022. "Current simulation with software in the loop for floating offshore wind turbines". *Journal of Physics: Conference Series,* ***2265***, 05, p. 042028.

[4] Gueydon, S., Bayati, I., and Ridder, E.-J., 2020. "Discussion of solutions for basin model tests of fowts in combined waves and wind". *Ocean Engineering,* ***209***, 08, p. 107288.

[5] ITTC, R. P., and Guidelines, 2021. 7.5 - 02 07 - 03.8 Model Tests for Offshore Wind Turbines. Tech. rep., International Towing Tank Conference, may.

[6] DNV-RP-0286, C. a. o. f. w. t., 2019. DNV-RP-0286 Coupled analysis of floating wind turbines. Tech. rep., DNVGL, may.

[7] Gueydon, S., Lindeboom, R., van Kampen, W., and de Ridder, E.-J., 2018. "Comparison of Two Wind Turbine Loading Emulation Techniques Based on Tests of a TLP-FOWT in Combined Wind, Waves and Current". Vol. ASME 2018 1st International Offshore Wind Technical Conference of *International Conference on Offshore Mechanics and Arctic Engineering*.

[8] Antonutti, R., Poirier, J.-C., and Gueydon, S., 2020. "Coupled Testing of Floating Wind Turbines in Waves and Wind Using Winches and Software-in-the-Loop". Vol. Day 2 Tue, May 05, 2020 of *OTC Offshore Technology Conference*.

[9] de Ridder, E.-J., Otto, W., Zondervan, G.-J., Huijs, F., and Vaz, G., 2014. "Development of a Scaled-Down Floating Wind Turbine for Offshore Basin Testing". Vol. 9A: Ocean Renewable Energy of *International Conference on Offshore Mechanics and Arctic Engineering*.

[10] Gueydon, S., Bayati, I., and Ridder, E.-J., 2021. "Oc6 semisubmersible response to waves in offset positions caused by constant thrust loads". *Journal of Physics: Conference Series,* ***2018***, 09, p. 012020.

[11] Journee, J., and Massie, W., 2001. *Offshore Hydromechanics*. Delft University of Technology.

[12] Koo, B., Goupee, A. J., Lambrakos, K., and Lim, H.-J., 2013. "Model Test Correlation Study for a Floating Wind Turbine on a Tension Leg Platform". Vol. 8: Ocean Renewable Energy of *International Conference on Offshore Mechanics and Arctic Engineering*.

[13] Gueydon, S., Judge, F. M., O'Shea, M., Lyden, E., Le Boulluec, M., Caverne, J., Ohana, J., Kim, S., Bouscasse, B., Thiebaut, F., Day, S., Dai, S., and Murphy, J., 2021. "Round robin laboratory testing of a scaled 10 mw floating horizontal axis wind turbine". *Journal of Marine Science and Engineering,* ***9***(9).

[14] Pires, O., Azcona, J., Vittori, F., Bayati, I., Gueydon, S., Fontanella, A., Liu, Y., Ridder, E.-J., Belloli, M., and Wingerden, J., 2020. "Inclusion of rotor moments in scaled wave tank test of a floating wind turbine using sil hybrid method". *Journal of Physics: Conference Series,* ***1618***, 09, p. 32048.

[15] Fontanella, A., Liu, Y., Azcona, J., Pires, O., Bayati, I., Gueydon, S., Ridder, E.-J., Wingerden, J., and Belloli, M., 2020. "A hardware-in-the-loop wave-basin scale-model experiment for the validation of control strategies for floating offshore wind turbines". *Journal of Physics: Conference Series,* ***1618***, 09, p. 32038.